

## IMPACT OF HIGH TEMPERATURE HEAT INPUT ON MORPHOLOGY AND MECHANICAL PROPERTIES OF DUPLEX STAINLESS STEEL 2205

Amol Y. CHAUDHARI<sup>1</sup>, Nilesh DIWAKAR<sup>2</sup> and Shyamkumar D. KALPANDE<sup>3</sup>

*The word "duplex" refers to the dual structure of austenite-ferrite stainless steels, which have exceptional mechanical and corrosion properties and are mostly employed for the production of parts for the marine industries. The harsh operating conditions at various temperatures in the marine industry may significantly reduce mechanical properties. The current work focuses on the morphological and mechanical properties of 2205 duplex stainless steel by multiple notches, higher temperature treatment at 1050°C, and different quenching media. Compared to other notches, the V notch treated specimen exhibits the highest impact toughness after air quenching. In terms of morphology, the volume percentages for the austenite phase during normalizing and the ferrite phase during quick quenching were almost the same, at 52-55%. The hardness analysis shows that an average value of up to 262 HV was obtained for the air cooled following heat treatment. The microstructure of DSS is not noticeably different in the furnace-cooled specimen. Due to the absence of secondary phases in rapidly cooled environments, the morphology of 2205 duplex stainless steel was marginally altered at higher temperatures, increasing the gauge length elongation for the specimen C up to 26.22%.*

**Keywords:** DSS 2205, Toughness, Tensile Strength, Micro hardness, Morphology, Heat treatment, Notch

### 1. Introduction

The name "duplex" refers to a dual structure of austenite-ferrite stainless steels, which have excellent mechanical and corrosion properties. As a result, there is an increasing trend toward the use of duplex 2205 stainless steels (DSSs) for the production of parts for the marine, chemical, oil and gas production, and pipeline industries that use various grades of stainless steel [1, 3]. Due to its excellent corrosion resistance, austenitic stainless steel is the most widely used steel [3].

The two primary alloying elements in DSSs are chromium (Cr) and nickel (Ni). The percentages of chromium and nickel in DSSs range from 4.5-8 and 4.18

<sup>1</sup> Ph.D. Research Scholar, SRK University, Bhopal, India

<sup>2</sup> Prof. Department of Mechanical, SRK University, Bhopal, India

<sup>3</sup> Prof. Department of Mechanical Engineering, GCOERC, Nashik, India

E-mail: camol1983@gmail.com

to 28 respectively [2]. The adjustment of austenite's immovability involves changing the proportions of nitrogen (N), carbon (C), manganese (Mn), and other alloying elements so that austenite's grains and grain boundaries undergo changes during deformation, improving the material's properties like strength and elongation [4, 5]. Mechanical properties and corrosion resistance depend on the precipitation and separation of the principal intermetallic phases and alloying components [6].

Since the transition from ductile to brittle diminishes impact strength but increases tensile properties, the presence of a ferritic phase in the morphology of DSS is directly related to the creation of ferrite crystal structure [7].

On the other hand, the austenitic phase's morphological appearance causes the impact properties of DSS to improve because it adapted permanent deformation and prevented low energy brittle fracture of the ferritic phase [5-7]. DSS is heated above its recrystallization temperature and cooled to ambient temperature in order to achieve the desired phase composition of ferrite and austenite with a phase balance of 50–50% [8, 9]. Their mechanical characteristics are largely explained by the percentage of intermetallic phases [2–6]. The proportions of the phases -ferrite, -austenite, and secondary phases like sigma - and chi - fluctuate in DSS as a function of temperature, and the morphology changes as ferrite, Ni, and Cr identical increase above the recrystallization temperatures [7].

When Cr, Mo, and S-silicon are present, the stable elements in ferrite increase the tendency for secondary phases like sigma ( $\sigma$ ) to develop. Molybdenum (mo), which has a higher percentage of the element than Cr, is able to promote the precipitation of the intermetallic phase more effectively than Cr, especially beyond the recrystallization temperature of 900°C [1, 6, 8, 10]. Although these elements can reduce the total percentage of ferrite phase as it is enhanced with Cr and Mo, they are crucial for austenite production in the morphology of the DSS and speed up the formation and development of the secondary phase. The components of the alloy are separated, and each component's intensity enhances the phases that cause the alloy to become stable. Consistent performance of the alloys in service conditions is greatly influenced by the appearance of various microstructural phases [13]. However, the development of secondary phases after cooling during heat treatment at temperatures ranging from 600°C to 900°C resulted in a significant loss of mechanical characteristics and corrosion resistance in the material [7, 8, 10, 14]. Another crucial factor was the intermetallic sigma () phase's high rate of development at 850 °C, which caused ferrite to disintegrate into the sigma ( $\sigma$ ) phase and the intermetallic austenitic phase [1, 5, 8, 15]. Sigma-, the most prevalent secondary phase, was used in even smaller levels (0.5%), which significantly reduced the resistance to cracking during impact tests [8, 14]. Body-centered tetragonal (BCT) crystal

structure dangerous undesirable secondary phase due to rapid phase creation and the main cause of corrosive qualities [1, 7, 8]. Sigma -phase's contribution to the microstructure is crucial in boosting hardness while lowering impact toughness and percentage of elongation [2, 6, 8]. Additionally, the fracture mode changed from individual bulk grain fracture to contiguous grain fracture based on the high degree of phase [16]. Intermetallic metastable chi-phase precipitates with ferrite-ferrite ( $\alpha + \alpha$ ) grain boundaries and body-centered cubic (BCC) crystal structure first arise before the sigma-phase formation [7, 11, 14]. Secondary sigma phase development can be seen at ferrite - ferrite ( $\alpha+\alpha$ ) interactions in addition to austenite - ferrite ( $\gamma+\alpha$ ) interfaces [8, 12].

It is clear from the research that the procedure of heat treatment and an adequate rate of cooling play a significant role in developing a state of phase equilibrium and in the improvement of the material's mechanical properties [4, 8, 11]. The proportion of ferrite gradually increased, and the percentage of austenite gradually reduced when the sample was heat treated at high temperatures between 1000 and 1250°C and rapidly cooled [18, 19]. Because the intermetallic sigma phase is brittle and hard, the hardness values are largely dependent on its presence or absence [1-3, 6, 20]. It is found in the morphological examination of DSS that cold distortion improves the mechanical properties [21-24].

The goal of the current experiment is to assess how the toughness, hardness, and morphology of duplex stainless steel 2205 change with and without heat treatment at 1050 °C and different quenching environments. The relationship between the morphology, impact toughness, tensile strength, and hardness of the steel at higher temperatures received special consideration.

## 2. Materials and Methods

The grade of duplex stainless steel 2205 used for the experiments is shown in Table 1 along with the percentage of each element's chemical composition. In the usual form of the Charpy impact test, 10 X 10 X 55 mm<sup>3</sup>, a total of nine specimens with various notches (specimen A, B, and C) were made. For the tensile test, 4 specimens were prepared. The specimen is heated to 1050°C in a muffle furnace, held there for 30 minutes, then quenched in one of three ways: 1) Water dilution to learn more about how high temperatures affect the microstructure, micro hardness, tensile strength, and toughness of materials, 2) Air quenching and 3) furnace quenching to atmospheric temperature (AT) have been used. The heat treatment circumstances used on the toughness specimen with various notches, as given in Tables 2 and Table 3, represent the treating environment for tensile specimens in this investigation. The Charpy impact toughness tests are carried out at room temperature using an impact toughness tester with a maximum energy of 300 J and an accuracy of 1 J. With a 1 kg

applied load, Vickers micro hardness is utilized to measure micro hardness. As indicated in Fig. 1, specimens for the tensile test are made with gauge lengths of 32 mm, gauge widths of 6 mm, and total lengths of 100 mm in accordance with ASTM E8.

The objective of the metallographic investigation is to clarify the morphological changes that take place in DSS. According to ASTM standards, the specimens are prepared for morphological analysis. The process of preparing a specimen requires a number of processes, including cutting, mounting, and wet-sanding the surface to a mirror sheen for the samples. The samples were cleaned with mineral water and then polished with Murakami's reagent, either through 10% oxalic acid solution for interpretation of grains and grain boundaries with an optical microscope or through immersion etchant to identify phases and prepare metallographic samples. After specimen preparation for microstructural analysis, the specimen was observed under compound microscope to spot the emergence of an intermetallic phase and to find out deformation changes in the ferrite and austenite phases. SEM is used to identify surface microstructure as well as to find out the morphological characteristics of austenite, ferrite, and intermetallic phases.

Table 1

**Chemical composition of 2205 DSS alloys (wt%)**

Elements	Cr	Ni	Mo	C	N	Mn	Fe
<b>Content</b>	22.37 %	5.48%	3.49%	0.021%	0.20%	1.370%	Balance

Table 2

**Notch, specimen identification and heat treatment**

Identification	Notch	Heat treatment
A1, B1, C1	V, U and keyway	without treatment
A2, B2, C2	V, U and keyway	1050 °C air cooling to room temperature (RT)
A3, B3, C3	V, U and keyway	1050 °C water cooling to room temperature (RT)

Table 3

**Tensile specimens and heat treatment**

Identification of tensile	Heat treatment
A	without treatment
B	1050 °C air cooling to room temperature (RT)
C	1050 °C water cooling to room temperature (RT)
D	1050 °C furnace cooling to room temperature

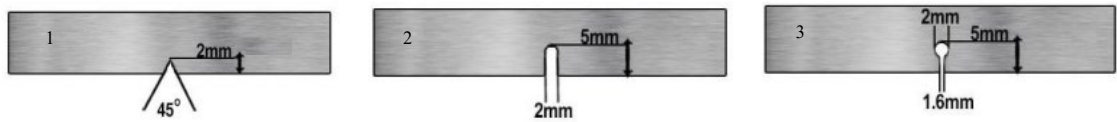


Fig. 1 Schematic diagram of the specimen for charpy impact test

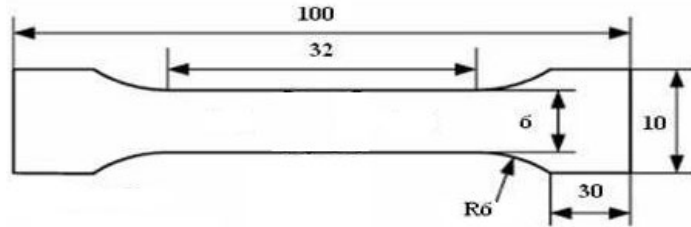


Fig 2. Schematic diagram of the specimen for tensile test

### 3. Results and discussion

The specimens A1, B1, and C1 are equivalent to those that have not undergone heat treatment; their morphology simply exhibits the appearance of ferrite and austenite phases, and intermetallic phases have not been added. possessing a fractional area where ferrite is 50.5% and austenite is 49.5%. The morphology of the material reveals ferrite to be darker in color than austenite. The temperature and length of aging, among other factors, affect the structure and quantity of the secondary phase fraction. After heat treatment, secondary phases may develop that alter the material's mechanical properties and corrosion resistance in a variety of situations [5, 13].

The material will move towards the precipitation of secondary phases through a thermodynamic stable state if DSS 2205 solution is treated below the recrystallization temperatures because the thermo chemical equilibrium of phases will break down [7, 11, 19]. Below 900 °C, the sigma phase was formed. Despite two concurrent transformations corresponding to the ferrite phase, secondary austenite production was free from the precipitation of the sigma phase.

Since the ferrite phase is unstable beyond the recrystallization temperature, secondary phases are created from nearby ferrites that have discriminatorily reacted at the ferrite  $\alpha$  / austenite  $\gamma$  or ferrite  $\alpha$  / ferrite  $\alpha$  boundary. These secondary phases differ by the organization of their microstructure and allocation.

#### 3.1 Microstructural morphology and distribution of phases

SEM analysis was used to determine how the heat treatment method affected the specimens' primary microstructure phase. The morphology of DSS specimens with and without heat treatment at 1050°C using various quenching mediums is shown in Fig. 3. Figure 3 (1) indicates that the studied specimen

solely contains the phases of  $\alpha$ -ferrite and  $\gamma$ -austenite present, with no subsequent precipitates. Figure 3 (2, 3, 4) shows the SEM morphology of specimens A2, B2, and C2 that have undergone thermal heat treatment with water quenching to atmospheric temperature (AT), air quenching to (AT) for specimens A3, B3, and C3, and furnace quenching to (AT) at 1050°C for 30 minutes, respectively. Due to the maximum transmission rates of dissolve alloys, ferrite is unbalanced in DSS at temperatures in the 600–900 °C range, and enriching ferrite with chromium and molybdenum causes a significant reduction in mechanical properties, which encourages the precipitation of secondary phases [4, 8, 15]. When subjected to recrystallization temperatures of 900 °C and higher,  $\gamma$ -ferrite forms a sigma-phase without first transitioning to an austenite phase, and the structure of the sigma-phase eventually transitions to a ferrite phase [13].

It illustrates that, heat treatment of specimens at this temperature is not responsible for the formation of intermetallic phases like sigma  $\sigma$  and chi  $\chi$  where they become  $\alpha$ -ferrite and  $\gamma$ -austenite. In the heat-treated specimen at 1050°C and water quenching to AT cooling shown in Fig. 3(3), the percentage of volume for the ferrite phase was 52-54%, while the austenite phase was seen at 52-55% in the treated specimen at 1050°C and air quenching to AT shown in Fig. 3(2).

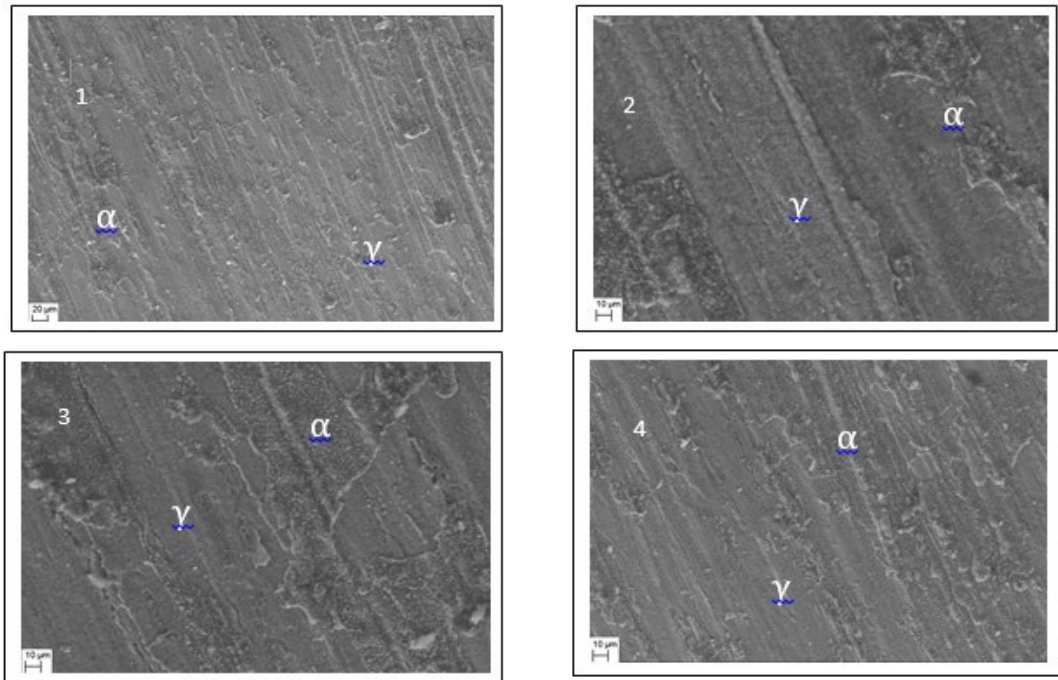


Fig 3. SEM image of the microstructure of (1) A Untreated specimen, (2) B air cooled specimen, (3) C water cooled specimen and (4) D furnace cooled specimen

### 3.2 Impact Strength

In order to ascertain the relationship between some of the mechanical features, a more thorough examination was completed. V-notch, U-notch, and keyway notches were dynamically tested for Charpy toughness; a notched specimen was struck by a swinging pendulum and fractured. The test specimens shall include three samples of each notch with the standard dimensions of 55 x 10 x 10 mm. A1, B1 and C1 are plane specimens of V, U and key way notch respectively. The specimens that have been heated to a temperature of 1050°C and then quenched in air or water to achieve AT are denoted by the letters A2, B2, C2, and A3, B3, C3, respectively.

The energy absorbed by the various notches and in various environments is depicted in Table 4. The plane specimen with the U notch and keyway notch had the lowest impact toughness, measuring 23 J. According to Fig. 3(1), the volume percentages for -ferrite and -austenite in plane specimens are 49.5% and 51.5%, respectively. The proportion of austenite was slightly higher in water-cooled specimens than in planar specimens. The coarse grains of ferrite in the specimens were cooled by water. The sample A2 (V notch) with air quenched to atmospheric temperature (AT) as shown in Fig 4 had the highest value of toughness, 33 J, after the heat treatment. This is unquestionably caused by the fine-grained effect of the crystal grain structure brought on by the slower cooling, as well as the normalization's increase in austenite volume percentage, which was close to 52–55%. Due to the precipitates of Cr2N present, preferential treatment should be given to the attack of the ferrite phase during water quenching of the specimen. In samples that are rapidly quenched, Cr and N elements also aid in the reduction of toughness in different notches [7, 9, 14, 15]. According to research, all normalized specimens exhibit greater toughness than untreated and water-quenched specimens, as indicated in Fig. 4. The lowest toughness was obtained in the untreated specimens of the all notches. From Fig. 4 it was observed that there was no considerable effect of notches on the impact toughness at high temperature heat treatment. According to the results of this experiment, the influence of high temperature heat treatment and quenching duration increased the specimens' toughness in all notches and prevented the formation of secondary phases.

Table 4  
Toughness of V, U and Keyway notch for different cooling medium

Cooling medium	V Notch		U Notch		Keyway Notch	
	Specimen	Toughness (J)	Specimen	Toughness (J)	Specimen	Toughness (J)
Plane	A1	24	B1	23	C1	23
A- Air Cooling	A2	33	B2	31	C2	30
W- Water Cooling	A3	27	B3	28	C3	26

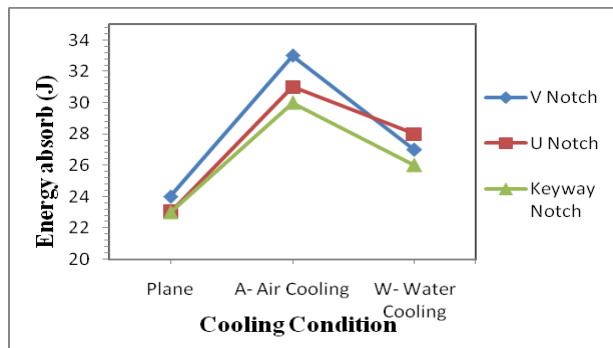


Fig. 4 Energy absorbed with different notch

### 3.3 Micro hardness

The three specimens (A, B, and C) underwent heat treatment and various quenching mediums to be evaluated for their micro hardness. The experimental results reveal that there are no appreciable changes in the hardness values for any of the specimens despite the presence of  $\alpha$ -ferrite and  $\gamma$ -austenite phases in the morphology of DSS. For DSS 2205, Table 5 details how the quenching medium used during the heat treatment affected the hardness. Vickers micro hardness values, which range from 255 to 278 HV for the specimens, depend on heating temperature at 1050 °C and quenching time for varied media. The normalizing specimen was heated to a temperature of 1050 °C, although this didn't have the greatest impact on the proportion of  $\alpha$ -ferrite and  $\gamma$ -austenite in the micro hardness. With increased heating temperatures and quick quenching, the hardness value for the heat-treated specimens changed.

Duplex stainless steel 2205 has a primary hardness for plain specimens of 255 HV, as indicated in Table 5. The average value of hardness for the plain and heat-treated specimens was also evaluated through heating at 1050 °C with various quenching media, presented in Fig. 5, as the primary factor of the mechanical properties. Intermetallic phases like the sigma  $\sigma$  phase that increase hardness are a result of heat treatment and quenching medium. It has been noted that the intermetallic sigma phase's hardness was significantly higher than major phases like  $\alpha$ -ferrite or  $\gamma$ -austenite [14]. The secondary sigma phase's presence or absence determines the hardness values [6, 8, 12]. The hardness of its primary and intermetallic phases was a major contributor to the hardness [10, 21, 23]. The major  $\gamma$ -austenite phase's hardness is dependent on the face-cubic crystal structure's deformation as a result of substitute mixed crystals made of big grain boundary elements like mo, Cr, and N [6, 11, 14]. In this experiment, all three untreated specimens (A, B, and C) were heated to a temperature of 1050 °C with air quenching and water quenching effects; as can be seen in Figure 3, none of the three specimens had secondary phases. Based on the severity of the stage in which the indentation occurs, a maximum quantity of hardness is determined. The hardness value shown in Fig. 5 does not represent a substantial change in harness

value since the heat treatment is not changed in this instance because there are no significant changes in the percentage of amount of phases present in the morphology of treated specimens with different quenching medium. The hardness test findings show that the annealing specimen has a maximum hardness value of 278 HV compared to the untreated and normalized specimen.

Table 5

Micro hardness for different cooling medium		
Samples	Cooling medium	Micro hardness HV
A	Plane	255
B	A- Air Cooling	262
C	W- Water Cooling	278

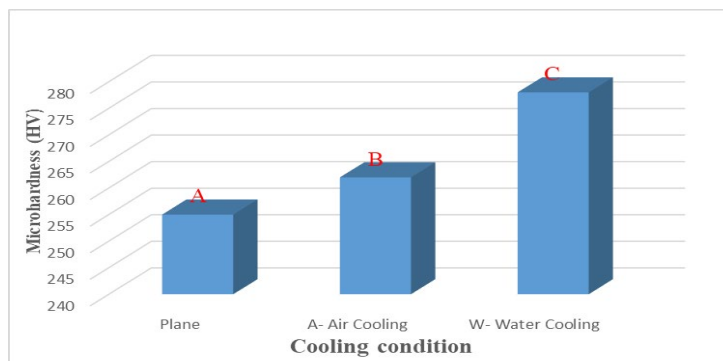


Fig. 5 Variation in micro hardness with cooling condition

### 3.4 Tensile Strength

The graphic depiction of the DSS 2205's tensile test for heat-treated and unheated coupons using various quenching media is presented in Fig. 6 (1-4). DSS 2205 is a duplex stainless steel that consists of a balanced microstructure of approximately equal amounts of ferrite and austenite phases. This unique microstructure provides the alloy with a combination of desirable properties such as high strength, good corrosion resistance, and improved resistance to stress corrosion cracking. The heat treatment process for DSS 2205 involves controlled heating and cooling cycles aimed at optimizing its microstructure and mechanical properties. The specific heat treatment parameters may vary depending on the desired outcome and the specific application requirements.

During the heat treatment process, the alloy is typically heated to a specific temperature within a range that promotes the dissolution of any secondary phases that may be present. Secondary phases in DSS 2205, such as sigma phase or intermetallic compounds, can adversely affect the material's mechanical properties, including its elongation and ductility. By carefully selecting the heat treatment temperature and duration, these secondary phases can be dissolved or minimized, leading to an improved microstructure with enhanced mechanical

properties. The heat treatment can also help refine the grain structure and relieve internal stresses within the material. The absence of secondary phases in the heat-treated DSS 2205 specimen indicates that the heat treatment process has been successful in preventing their formation or eliminating them if present initially. This absence contributes to the improved mechanical properties of the alloy.

Now, let's focus on the high elongation observed during the breaking of the heat-treated DSS 2205 specimen as shown in Fig. 6. Elongation is a measure of a material's ability to deform plastically before fracture and is typically expressed as a percentage increase in gauge length during a tensile test. The high elongation observed suggests that the heat-treated DSS 2205 specimen possesses good ductility. Ductility refers to the ability of a material to undergo plastic deformation without fracturing and is an essential property for applications where the material may be subjected to high stress or deformation. Several factors contribute to the high elongation of the heat-treated DSS 2205 specimen. First, the balanced ferrite-austenite microstructure of DSS 2205 inherently provides a good combination of strength and ductility. The ferrite phase contributes to strength, while the austenite phase offers ductility and toughness. Additionally, the heat treatment process can refine the grain structure, reduce the presence of impurities, and relieve stresses within the material, all of which contribute to improved ductility and elongation.

In summary, the heat treatment of DSS 2205 aims to optimize its microstructure and mechanical properties. The absence of secondary phases achieved through the heat treatment process, combined with the inherent balanced microstructure of the alloy, leads to improved mechanical properties, including high elongation during breaking. This indicates enhanced ductility and toughness, making the material suitable for demanding applications requiring deformation resistance and resistance to fracture.

Table 6 shows the tensile test findings, in the present case a load displacement curve does not exhibit a distinct yielding plateau or a well-defined linear zone, the yield strength is determined by the 0.2% proof stress. In the absence of a distinct yield point or linear zone, the 0.2% proof stress is utilized as an alternative method. On the curve, this method involves measuring the load at a specified displacement value (typically 0.2%). Typically, this value is determined by drawing a line parallel to the initial linear portion of the curve and locating the load value at the intersection of this line with the curve. If the curve does not clearly exhibit yielding behavior, the material may exhibit strain hardening or other complex deformation mechanisms.

As shown in Fig. 7 (1), it was observed that the percentage of elongation in heat-treated and water-cooled samples was 26.22% higher than that in untreated, air-cooled, and furnace-cooled samples. Untreated specimens showed the least change in gauge length (12.8 mm), while water-cooled specimens

showed the most change in gauge length (13.11 mm), as shown in Fig. 7 (2). Fig. 3's morphology of the treated specimens reveals no instances of secondary phase. While the impact toughness and tensile strength are likewise noticeably reduced, the hardness is significantly improved by the  $\alpha$ -phase [4, 8, 14].

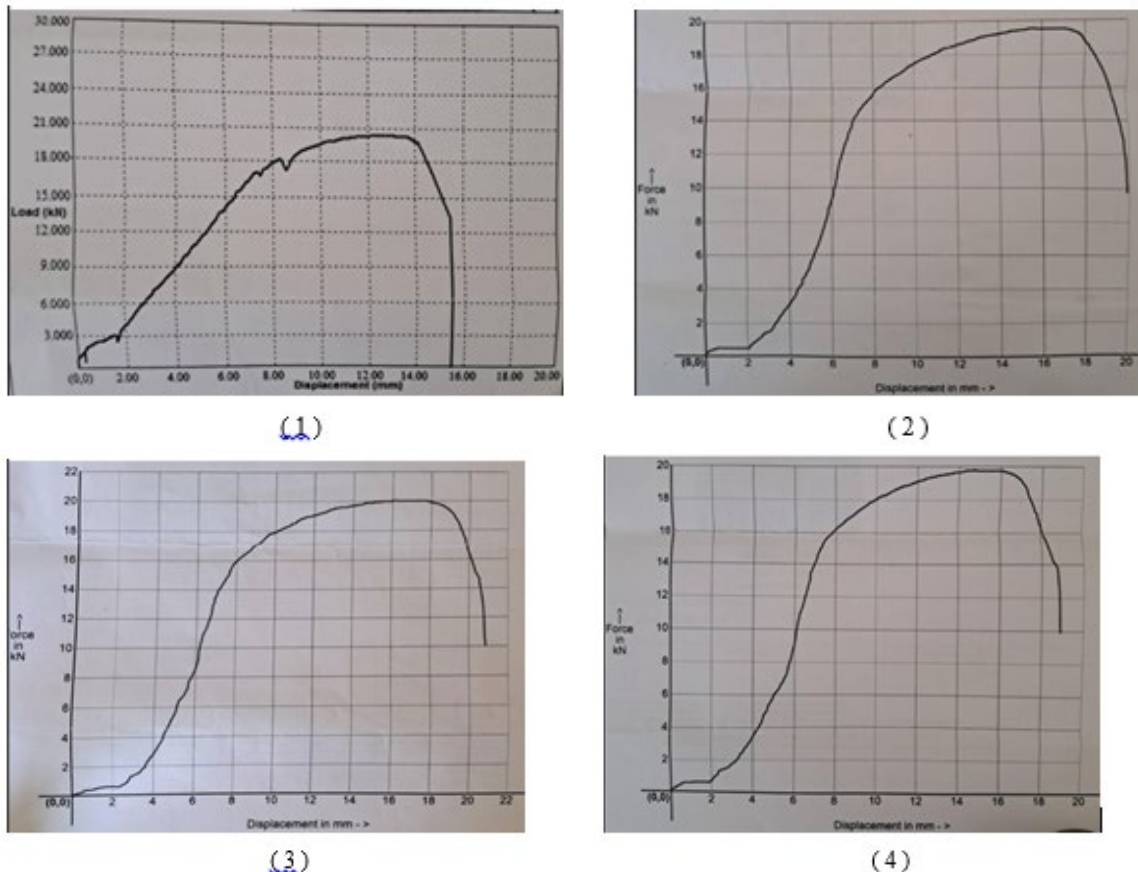


Fig. 6 Load vs. displacement curves (1) Plane sample (2) Air Cooled (3) Water Cooled (4) Furnace cooled

Table 6

Result of Tensile Test Properties

Samples	Cooling Medium	% of Elongation	Change in Gauge Length (mm)	Tensile Strength (MPa)	Yield Strength (MPa)
A	Plane	19.35	12.8	701.75	460
B	A- Air Cooling	24.52	13	705.35	530.34
C	W- Water Cooling	26.22	13.11	730.4	565
D	F- Furnace Cooling	22.66	12.9	690	543.73

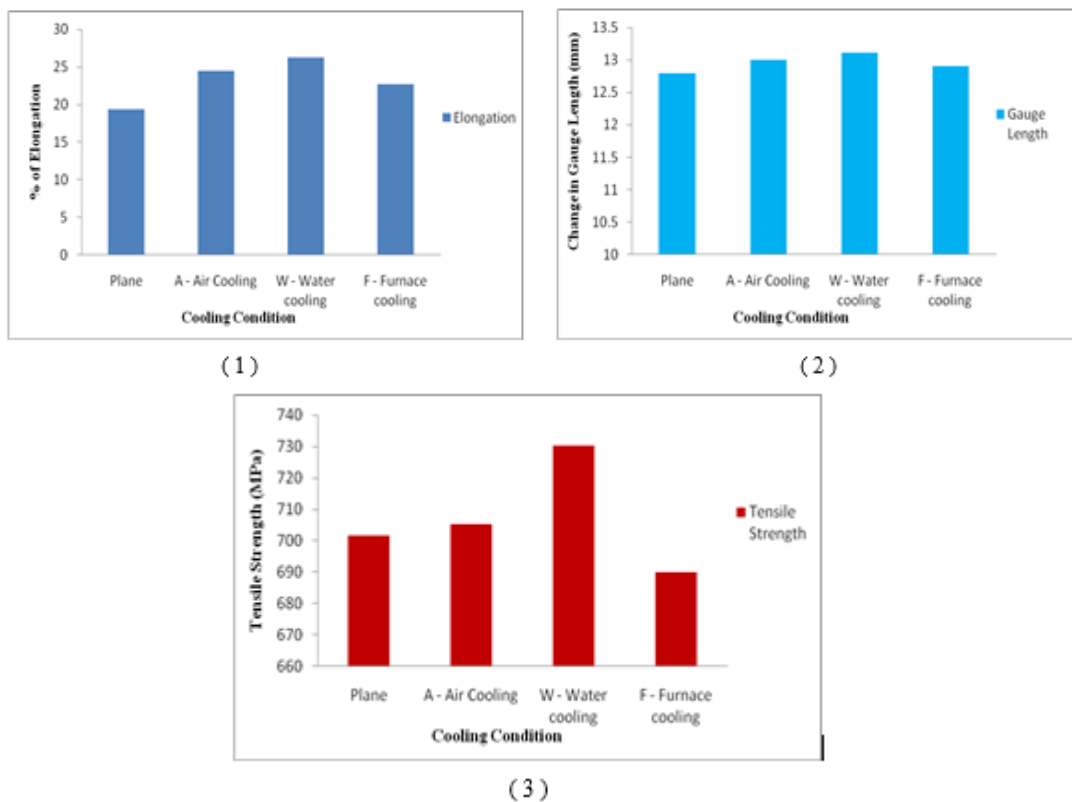


Fig. 7 Graphical Representation of (1) % of elongation (2) Change in gauge length (mm) (3) Tensile strength (MPa)

In comparison to untreated and furnace cooled specimens illustrated in Fig. 3 (1-4), there was a modest shift in the volume proportion of ferrite and austenite in heat treated specimens quenched in water and air. In comparison to samples A, B, and D, the yield strength of sample C increased to 565 MPa, as indicated in Table 6. The sample C's morphology changed as a result of being heated to 1050°C and quickly cooled at AT. This treatment increased the proportion of ferrite phase by up to 52–54%, which helped the material's tensile strength, as shown in Fig. 3(3). According to Fig. 7 (3), specimen C exhibits a maximum tensile strength of 730.40 MPa when compared to other samples as the percentage of ferrite increases.

#### 4. Conclusions

The objective of this research is to investigate the impact of notches and heat treatment procedures on the morphology, impact toughness, micro hardness, and tensile strength of DSS 2205 at high temperature 1050°C by various quenching media. The main observations made as a result of the investigations are listed below.

1. Impact of high temperature heating, different quenching media and quenching time plays an important role in balance the percentage volume of components and formation of intermetallic phase and equilibrium phases in DSS 2205.
2. The microhardness of DSS 2205 was not significantly affected by the heat treatment carried out at 1050°C because the intermetallic  $\sigma$  and  $\chi$  phases were not found in the material.
3. The micro hardness results revels that annealed specimen shows maximum hardness that is up to 278 HV higher than the untreated and normalizing specimen.
4. From the results of impact toughness it is observed that normalizing of V-notch specimen shows highest value of toughness 33J and an increase in the volume percentage of austenite by 52-55% as compared to U and keyway notch in plane and rapid cooled specimens.
5. The percentage of ferrite phase increases up to 52-54%, which is helpful for enhancing the tensile strength up to 730.40 MPa due to microstructural changes in the sample C heated to 1050°C and rapidly quenched at AT.

## R E F E R E N C E S

- [1] *H. Li, L. Zhang, B. Zhang and Q. Zhang*. "Effect of heat treatment on the microstructure and corrosion resistance of stainless/carbon steel bimetal plate". Advances in Materials Science and Engineering 2020, pp. 1-12.
- [2] *A. Y. Chaudhari & D. D. Deshmukh*. "Metallurgical investigations on corrosion behavior of simple and heat treated duplex stainless steel 2205 exposed to corrosive media". IOP Conference Series: Materials Science and Engineering, **Vol. 810** (1), 2020, pp. 012048.
- [3] *L. Jerzy, A. Swierczyńska and S. Topolska*. "Effect of microstructure on mechanical properties and corrosion resistance of 2205 duplex stainless steel". Polish Maritime Research **Vol. 21** (4), 2014, pp. 108-112.
- [4] *M. Pan, X. Zhang, P. Chen, X. Su and R. Misra*. "The effect of chemical composition and annealing condition on the microstructure and tensile properties of a resource-saving duplex stainless steel". Materials Science and Engineering: A, **Vol. 788**, 2020, pp.139540.
- [5] *A. S. Hamood, A. F. Noor and M. T. Alkhafagy*. "Effect of heat treatment on corrosion behavior of duplex stainless steel in orthodontic applications". Materials Research Express, **Vol. 4** (12), 2017, pp.126506.
- [6] *M. B. Davanageri, S. Narendranath and R. Kadoli*. "Influence of Heat Treatment on Microstructure, Hardness and Wear Behavior of Super Duplex Stainless Steel AISI 2507". American Journal of Materials Science, **Vol. 5** (3C), 2015, pp. 48-52.
- [7] *C. Gennari, L. Pezzato, E. Piva, R. Gobbo and I. Calliari*. "Influence of small amount and different morphology of secondary phases on impact toughness of UNS S32205 Duplex Stainless Steel". Materials Science and Engineering: A, **Vol. 729**, 2018, pp.149–156.
- [8] *C. Paulsen, R. Broks, M. Karlsen, J. Hjelen and I. Westermann*. "Microstructure evolution in super duplex stainless steels containing  $\sigma$ -phase investigated at low-temperature using in situ SEM/EBSD tensile testing". Metals, **Vol. 8** (7), 2018, pp. 478.
- [9] *N. Haghadi, P. Cizek, P. D. Hodgson and H. Beladi*. "Microstructure dependence of impact toughness in duplex stainless steels". Materials Science and Engineering, 745, 2019, pp. 369-378.

- [10] *G. Argandoña, J. Palacio et al.* “Effect of the temperature in the mechanical properties of austenite, ferrite and sigma phases of duplex stainless steels using hardness, micro hardness and nano indentation techniques”. *Metals*, **Vol. 7** (6), 2017, pp. 219.
- [11] *S. Li, W. Ding, Q. Zhang, X. Xiao and Q. Zhou.* “Experimental study of the mechanical properties of a new duplex stainless steel exposed to elevated temperatures”. *Case Studies in Construction Materials*, **Vol. 17**, 2022.
- [12] *M. Mehta, P. Jadhav, A. Shaikh, S. Kumar and S. Kirwai.* “Effect of Solution Treatment on Microstructure and Mechanical Properties of 2205 Duplex Stainless Steel”. *International Journal of Manufacturing, Materials, and Engineering*, **Vol. 7** (6), 2019.
- [13] *Z. Wu, Y. F. Cheng, L. Liu, W. Lu and W. Hu.* “Effect of heat treatment on microstructure evolution and erosion-corrosion behavior of a nickel-aluminum bronze alloy in Chloride Solution”. *Corrosion Science*, **Vol. 98**, 2015, pp.260–270.
- [14] *S. Topolska and J. Labanowski.* “Impact-toughness investigations of duplex stainless steels”. *Materials Technology*, **Vol. 49** (4), 2015, pp. 481–486.
- [15] *D. S. Kahar.* “Duplex Stainless Steels-an overview”. *International Journal of Engineering Research*, **Vol. 07** (04), 2017, pp.27–36.
- [16] *M. A. Makhdoom, A. Ahmad, M. Kamran, K. Abid and W. Haider.* “Microstructural and electrochemical behavior of 2205 duplex stainless steel weldments”. *Surface and Interface Analysis*, **Vol. 9**, 2017, pp. 189–195.
- [17] *X. Guo, T. Li, Z. Shang, Y. Zhu and G. Li.* “The precipitation behavior of second phase in high titanium microalloyed steels and its effect on microstructure and properties of steel”. *High Temperature Materials and Processes*, **Vol. 41**, 2022, pp.111-122.
- [18] *D. D. Deshmukh and V. D. Kalyankar.* “Deposition characteristics of multitrack overlayby plasma transferred arc welding on ss316lwith co-cr based alloy – influence of process parameters”. *High Temperature Materials and Processes*, **Vol. 38**, 2019, pp. 248–263.
- [19] *K. A. Abdelazem, H. M. El-Aziz, M. M. Ahmed and I. G. El-Batanony.* “Characterization of mechanical properties and corrosion resistance of SAF 2205 duplex stainless steel groove joints welded using friction stir welding process”. *International Journal of Recent Technology and Engineering*, **Vol. 8** (6), 2020, pp. 3428–3435.
- [20] *T. H. Chen, K. L. Weng and J. R. Yang.* “The effect of high-temperature exposure on the microstructural stability and toughness property in a 2205 duplex stainless steel”. *Materials Science and Engineering: A*, **Vol. 338** (1-2), 2002, pp. 259–270.
- [21] *V. D. Kalyankar and D. D. Deshmukh.* “On the performance of metallurgical behaviour of stellite 6 cladding deposited on SS316L substrate with PTAW process”. *Canadian Metallurgical Quarterl*, **Vol. 61** (2), 2022, pp. 130–144.
- [22] *D. D. Deshmukh and V. D. Kalyankar.* “Analysis of deposition efficiency and distortion during multitrack overlay by plasma transferred arc welding of Co–CR alloy on 316L Stainless Steel”. *Journal of Advanced Manufacturing Systems*, **Vol. 20** (04), 2021, pp. 705–728.
- [23] *A. Y. Chaudhari, N. Diwakar and S. D. Kalpande.* “Effect of heat treatment on microstructure, mechanical and corrosion characteristics of Duplex Stainless Steel 2205: A Review”. *scope*, **Vol. 13** (01), 2023, pp. 301-313.
- [24] *L. Pezzato, M. Lago, K. Brunelli, M. Breda and I. Calliari.* “Effect of the heat treatment on the corrosion resistance of Duplex Stainless Steels”. *Journal of Materials Engineering and Performance*. **Vol. 27** (8), 2018, pp. 3859–3868.